(32) Patel, B. M.; Winefordner, James D. *Spectrochim. Acta* **1986**, *41B*, 469-474.
(33) Gough, David S.; Meldrum, J. R. *Anal. Chem.* **1980**, *52*, 642-646.
(34) Smith, B. W.; Omenetto, Nicolo; Winefordner, James D. *Spectrochim. Acta* **1986**, *39B*, 1389-1393.
(35) Harrison, Willard W.; Hess, Kenneth R.; Marcus, R. Kenneth; King, Fred L. *Anal. Chem.* **1986**, *58*, 341A-356A.
(36) Hess, Kenneth R.; Harrison, Willard W. *Anal. Chem.* **1986**, *58*, 1696-1702.
(37) Harrison, Willard W.; Bentz, B. L. *Prog. Anal. Spectrosc.* **1988**, *11*, 53-110.
(38) Duckworth, Douglas C.; Marcus, R. Kenneth *Anal. Chem.* **1989**, *61*, 1879-1886.
(39) Westwood, W. D. *Prog. Surf. Sci.* **1976**, *7*, 71-111.
(40) Fang, D.; Marcus, R. Kenneth *Spectrochim. Acta* **1988**, *43B*, 1451-1460.
(41) Stocker, B. J. *Br. J. Appl. Phys.* **1961**, *12*, 465-468.
(42) Chapman, Brian *Glow Discharge Processes*; John Wiley & Sons: New York, 1980.
(43) Hannaford, Peter; Walsh, Alan *Spectrochim. Acta* **1988**, *43B*, 1053-1068.
(44) L'vov, Boris V. *Atomic Absorption Spectrochemical Analysis*; Adam Hilger: London, 1970.
(45) Bernhard, Alan E.; Khan, H. L. 35th Canadian Spectroscopy Conference, **1988**, Paper No. 67.
(46) Chang, Shye-Bin; Chakrabarti, Chuni L. *Prog. Anal. Atom. Spectrosc.* **1985**, *8*, 83-191.
(47) L'vov, Boris V.; Nikolaev, V. G.; Norman, E. A.; Polzik, L. K.; Mojica, M. *Spectrochim. Acta* **1986**, *41B*, 1403-1053.
(48) Piepmeier, Edward H. *Spectrochim. Acta* **1989**, *44B*, 609-616.
(49) Wagenaar, H. C.; Novotný, I.; de Galan, Leo *Spectrochim. Acta* **1974**, *29B*, 301-317.
(50) Unpublished work, Carleton University, 1989.

RECEIVED for review July 11, 1989. Accepted December 5, 1989. The authors are grateful to the Natural Sciences and Engineering Research Council of Canada (NSERC) for financial support of this research project. J. C. Hutton is also grateful to NSERC for the award of a postgraduate scholarship. Part of this paper was presented as an invited keynote paper at the XXVI Colloquium Spectroscopicum Internationale, July 2-9, 1989, Sofia, Bulgaria.

Long Path Atomic/Ionic Absorption Spectrometry in an Inductively Coupled Plasma

Michael A. Mignardi, Benjamin W. Smith, and James D. Winefordner*

Department of Chemistry, University of Florida, Gainesville, Florida 32611

A novel approach was taken to increase the atomic/ionic absorption path length in an inductively coupled plasma (ICP) by using a water-cooled quartz "T-shaped" bonnet. Atomic and ionic absorption spectrometry was performed utilizing a continuum source and line sources. Absorption spectra of synthetic multielement solutions were collected with a photodiode array. Sample introduction into the ICP was accomplished with an ultrasonic nebulizer. To prevent the bonnet from cracking, low radio frequency powers were utilized (i.e., 400-600 W). Plasma diagnostics were performed to study the plasma temperature and electron number density within the "T-shaped" bonnet. Analytical figures of merit were found to be better than those obtained from previous work attempted with inductively coupled plasma atomic absorption spectroscopy and approaching that of flame atomic absorption spectroscopy.

INTRODUCTION

Since the beginning of flame atomic absorption spectrometry (AAS), several workers have tried to enhance the analytical sensitivity by increasing the absorption path length of the atomic absorption reservoir (*1*). Fuwa and Vallee performed a study of the Beer-Lambert law for absorption of molecules in solution as a model for the investigation of atomic absorption (*2*). In their work, a long path absorption cell (90-250 cm) was made of Vycor for flame AAS. The combustion flame burner was positioned such that the tail flame was directed into one end of the absorption cell. Source radiation from a hollow cathode lamp (HCL) passed through the absorption cell and then through focusing optics onto a spectrograph. Compared to conventional flame AAS, they were able to increase the sensitivity for some elements by about 2 orders of magnitude (*2*, *3*). Other work using this long path absorption cell showed that the diameter and reflection from the inner walls of the absorption tube affect the absorbance (*4*). The smaller the diameter (up to 1 cm), the higher will be the concentration of absorbing atoms and hence the higher the absorbance (*2*, *4*). Earlier stages of the work by Fuwa and Vallee involved placing the tube in a "T-shaped" fashion over the flame burner and thus deflecting the flame in two directions (rather than in one direction as previously done) (*2*); however, this system failed to yield satisfactory results with AAS. Rubeska also used Fuwa long absorption cells in a T-shaped fashion over a flame. In this setup, the absorption cell was electrically heated so as to increase the mean lifetime of free atoms (*1*). With the long path absorption cell, good sensitivities were obtained and the formation of oxides for some elements was reduced since the tube shielded the flame gases from the oxidizing atmosphere.

Most work in AAS has utilized flames and electrothermal atomizers as the atom reservoirs. The choice of an atom reservoir and its atomization efficiency is obviously one of the most important considerations in AAS. Compared to flames and electrothermal atomizers, argon inductively coupled plasmas (ICPs) are excellent vaporization, atomization, excitation, and ionization sources for atomic spectroscopy. Several attractive properties of the ICP are (i) high plasma temperatures and number density of free electrons, (ii) longer residence times of free atoms in an inert chemical environment, and (iii) reduced formation of chemical compounds (e.g., refractory compounds) (*5-8*). There are, however, several disadvantages (*9*, *10*): (i) large dilution of gaseous analyte atoms; (ii) small absorption path length; (iii) ionization losses (i.e., a smaller atom ground state population); (iv) a broad continuum spectral background; and (v) higher cost and difficulty of operation compared to flames and electrothermal atomizers. Because of these disadvantages, analytical work in ICP-AAS has been limited.

In 1966, Wendt and Fassel attempted to overcome the small absorption path length in ICPs by utilizing a multipass system for ICP-AAS (*7*). In their setup, a collimated beam from an

* To whom correspondence should be sent.

0003-2700/90/0362-0586$02.50/0

HCL made three passes through an ICP with mirrors placed around the plasma and then into a spectrometer. They achieved detection limits and sensitivities comparable to the best reported flame-AAS values at that time. Veillon and Margoshes uses a modified Wendt and Fassel ICP torch (without the most central concentric tube) in a single-pass system with a modulated source and phase sensitive amplifier (*8*). They did not observe some of the chemical interferences commonly observed in flames. Biancifiori and Bordonali, using a single-pass ICP-AAS system, also noticed a decrease in chemical interferences compared to flame-AAS (*11*, *12*); their ICP configuration consisted of an absorption chamber inserted into a single torch tube having a length much longer than usual. Veillon and Margoshes concluded that except for a few refractory elements, the ICP did not appear to be a suitable replacement for the chemical flame in AAS. Like Fuwa and Vallee, Greenfield conducted work involving a physical increase in the absorption path length, but, in an ICP (*13*). Greenfield was able to extend the outer sheath of the ICP torch to 60 cm and later found he was able to bend the extended plasma "tail flame" at right angles. Ultimately, the outer sheath of the ICP took on the shape of a "T". When one end of the T was closed with an optical flat, the plasma tail-flame was forced to turn away from the optical flat. A modulated HCL was collimated and sent through the optical flat and into a spectrometer near the open end of the T. Temperatures within the T ranged from 3000 to 8000 K. The high-temperature plasma in the T should minimize chemical interferences due to the formation of stable refractory compounds of the element under investigation. Because of the extended probe region above the ICP load coil, the potential for spectral emission interferences was greatly reduced. Also, a lower background radiation was observed by the tail-flame, thus indicating an advantage over combustion flames in AAS.

A decade later, Abdallah et al. (*14*) and Mermet and Trassy performed work on increasing the absorption path length in a ICP (*10*). Here, the absorption path length was increased by having the light beam pass through the plasma channel along the symmetry axis. The plasma torch was turned on its side and a beam of radiation, focused with a lens at the base of the torch, was sent down the torch axially. The outer sleeve of the torch was extended to further enhance the lifetime of neutral atoms in the plasma. They achieved detection limits and sensitivities competitive with flame-AAS and approaching those of electrothermal atomizers. Other work by Magyar and Aeschbach involved removing the atomization cell from a commercial AA instrument and replacing it with an ICP (*6*). The enhanced atomic emission signal from the ICP made it necessary to use higher intensity HCLs than for flame-AAS. Their results indicated the possible use of ICP-AAS for the determination of metals in complex compounds, which do not efficiently dissociate in combustion flames. Downey and Nogar performed intracavity dye laser absorption spectrometry (IDLAS) by placing an ICP within the cavity of a pulsed, flashlamp-pumped dye laser for AAS. They achieved an enhancement factor of approximately 170 relative to single-pass absorption in an ICP (*9*). Limits of detection (LODs) in the parts-per-million range were obtained for sodium and barium. These workers were able to take advantage of the ICP as an ion source. The tunability of the dye laser allowed investigation of barium ion, Ba(II), absorption at 614.1 nm. Umemoto and Kubato performed ionic absorption spectrometry of scandium in an ICP. In their setup, collimated radiation from a continuum source made two passes through the ICP and into a high-resolution spectrometer. They performed diagnostic studies of the effect of plasma height and radio frequency (rf) power on ionic absorbance. The detection limits they achieved were comparable to ICP-AES (*15*). Several workers have also performed some successful fundamental studies on ICP argon chemistry and plasma diagnostics using atomic and ionic absorption spectrometry (*16–23*). In these studies, continuum sources, HCLs, microwave induced plasmas, and ICPs were used as radiation sources.

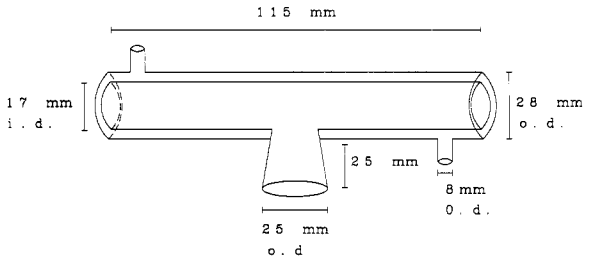

Figure 1. Detailed drawing of T-shaped bonnet.

Recently, Blades and Ng have independently performed atomic absorption studies using long absorption path lengths. Liang and Blades achieved excellent sensitivities utilizing an atmospheric pressure capacitively coupled plasma and a T-shaped device (*24*). Ng et al. achieved sensitivities comparable to the work performed by Aeschbach utilizing long path absorption within the Beenakker cavity of a microwave-induced plasma (*25*).

In this work, further investigation has been performed utilizing an ICP for AAS studies. An attempt to increase the absorption path length of the ICP was made with the design of a cooled-quartz T-shaped bonnet for the ICP. Unlike Greenfield's T-shaped torch, this bonnet was detachable from the torch, positioned closer to the load coil, and water cooled. A detailed description of the T-shaped bonnet is given. An evaluation of this T-shaped bonnet was performed by atomic and ionic absorption spectrometry in an ICP for pure and multielement synthetic solutions with a continuum source and several line sources (HCLs). Analytical figures of merit and plasma diagnostics (plasma temperature and electron number densities) are given as well.

EXPERIMENTAL SECTION

Design and Construction of the T-Shaped Bonnet. A detailed drawing of the T-shaped bonnet is shown in Figure 1. The bonnet was constructed within our glass shop of Spectrosil quartz tubing (Thermal American Fused Quartz, Monteville, NJ). Tubing for the T portion consisted of two concentric tubes. The tubing used for the outside portion of the T was 25 mm i.d. and 28 mm o.d., and the tubing used for the inside portion of the T was 17 mm i.d. and 19 mm o.d. These two tubes were fused together at their ends so as to create a water jacket between them. The length of the T was 115 mm. The tubing for the stem of the T was 22 mm i.d. and 25 mm o.d. and was 25 mm long. Intake and return of chilled water to the T-shaped bonnet was via 6 mm i.d. and 8 mm o.d. tubing. Chilled water to the bonnet was kept at ≤5 °C (Neslab Instruments, Inc., Portsmouth, NH). The flow rate of water to the bonnet was 7–11 L h^{-1}. The T-shaped bonnet was mounted in two nylon clamps attached to an X,Y,Z-translation axis mount such that the T-shaped bonnet could be carefully positioned on top of the ICP. Figure 2 is a diagram of the bonnet within the nylon clamps. The ICP torch was also mounted on an X,Y,Z-translation axis mount such that the torch could be properly positioned within the T-shaped bonnet. Translation of both the ICP torch and bonnet allowed easy manipulation of the setup and the ability to optically probe different regions within the T.

Plasma Operation. Before plasma ignition, chilled water was allowed to flow through the T-shaped bonnet and ICP load coil for approximately 5 min to ensure that the bonnet was properly cooled. Ignition of the plasma with the torch inside the T-shaped bonnet was difficult; therefore, before plasma ignition, the ICP torch had to be lowered such that the bottom of the bonnet stem was at least 20 to 25 mm above the top of the outer sheath of the torch. Once the plasma was ignited in this lowered position, the

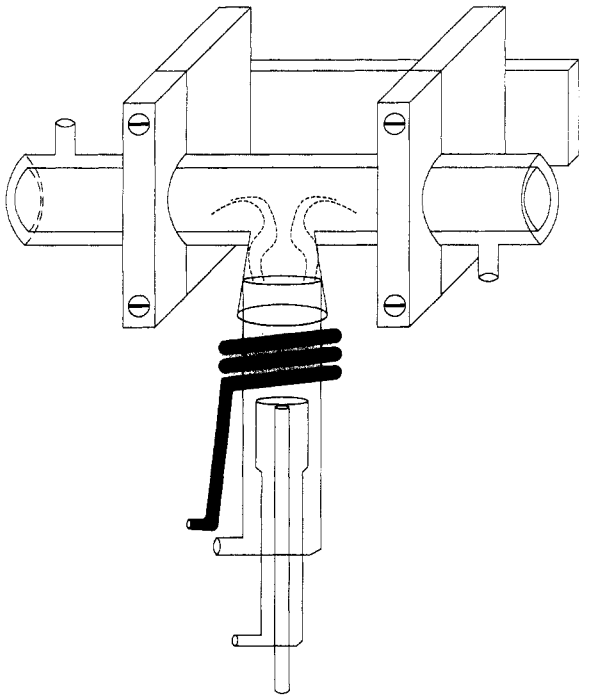

Figure 2. Diagram of ICP torch and bonnet.

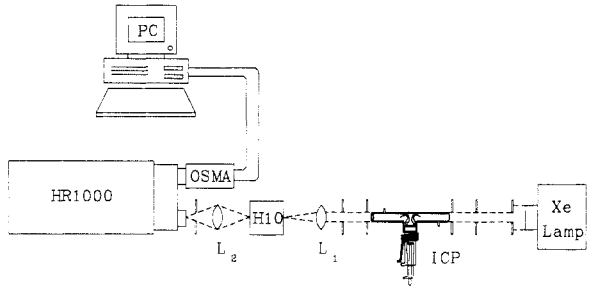

Figure 3. Schematic diagram of CS-ICP-AAS experimental setup.

torch was then slowly raised into the T-shaped bonnet until the center of the longitudinal T portion of the bonnet was approximately 27 mm above the torch load coil. Figure 2 also shows the ICP torch positioned within the T-shaped bonnet during operation. Once in position, the torch was operated as usual. The torch was operated at low powers (i.e., 400–600 W) so as not to overheat and possibly crack the T-shaped bonnet. At these low ICP powers, this experimental setup could be run continuously (the maximum continuous operation at one time was 8 h).

After extended use of this experimental system, and especially after aspiration of high salt concentration into the plasma, an oxide formation was observed within the inner wall of the T-shaped bonnet. Despite this residue formation, there were no analyte memory effects observed within the system. After periodic use, the T-shaped bonnet was removed and immersed in a 10% HNO_3 solution to clean the inner walls of the bonnet. No vitrification of the quartz tubing was observed. Since the T-shaped bonnet is made of quartz, the bonnet acted like a light-pipe; i.e., the plasma continuum emission was reflected from the ends of the bonnet. Most of this plume emission was spatially discriminated against by using appropriate apertures.

Instrumentation. Figures 3 and 4 are schematic diagrams of the optical arrangements used in this work for the continuum and line sources, respectively. The optical probing of atomic and ionic species within the center of the T-shaped bonnet was 27 mm above the ICP load coil. The instrumentation and experimental operating conditions for the continuum source studies were previously described (26). Table I is a list of the instrumentation and operation parameters for the HCL-ICP-AAS studies. All optics used in both setups (see Figures 3 and 4) were of fused silica.

For the HCL-ICP-AAS studies, a 1:1 image of the HCL emission was focused onto a chopper wheel with lens 1, L_1 (5 cm focal length and diameter). A 1:1 image from the chopper wheel to the center

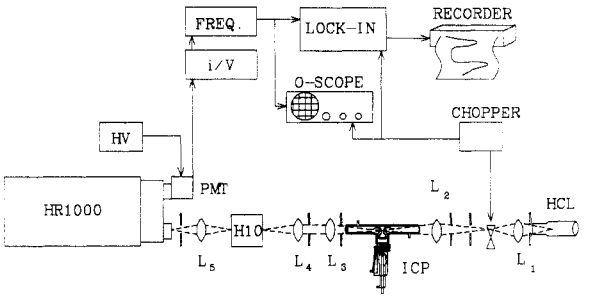

Figure 4. Schematic diagram of HCL-ICP-AAS experimental setup.

Table I. Instrumentation and Operating Parameters for HCL-ICP-AAS

instrumentation	manufacturer and operating parameters
I. ICP	
rf power supply	Plasma-Therm, Inc., Kresson, NJ, Model HPF 2000D
rf frequency	27.12 MHz
forward rf power	400–600 W
reflected rf power	0–20 W
Ar coolant flow rate	14 L min^{-1}
Ar auxiliary flow rate	1.5 L min^{-1}
Ar carrier flow rate	0.9 L min^{-1}
observation height[a]	27 mm
II. ultrasonic nebulizer	
rf power supply	Plasma-Therm, Inc.
rf frequency	1.35 MHz
forward power	37 W
reflected power	3 W
III. HCL	Fisher Scientific, Springfield, NJ
power supply	Heath Co., Benton Harbor, MI, Model EU-703-62
lamp current	3–8 mA
IV. monochromators	Instruments SA, Inc., Metuchen, NJ
predisperser	Jobin-Yvon H10
grating	1200 grooves mm^{-1}
slits	2 mm
linear dispersion	8 nm mm^{-1}
high resolution	Jobin-Yvon HR1000
grating	2400 grooves mm^{-1}
linear dispersion	0.5 nm mm^{-1}
slits	1–2 mm
V. optical chopper	Photon Technology International, Inc., Princeton, NJ, Model OC 4000
modulation frequency	200 Hz
VI. readout	
current amplifier	Keithley Instruments, Inc., Cleveland, OH, Model 427 1 ms rise time, 10^4 V A^{-1}
nanovolt amplifier	Keithley, Model 103A 100–300 Hz bandwidth, 100 gain
lock-in amplifier	Princeton Applied Research Corp., Princeton, NJ, Model 186A, 3 s time constant, 1 kHz low-pass filter
strip chart recorder	Fisher Scientific, Recordall, Model 5000

[a] Measured above the load coil.

of the T-shaped bonnet (27 mm above the axial center of the ICP load coil) was made using L_2 (13 cm focal length and 2 cm diameter). The focused radiation at the center of the bonnet was collimated with L_3 (23 cm focal length and 2.5 cm diameter). L_4 (5 cm focal length and diameter) focused the collimated radiation onto the 2-mm entrance slit of the predisperser monochromator. The predisperser minimized any higher orders of emission radiation from the ICP. A 1:1 image from the exit slit of the predisperser was formed at the entrance slit of the HR1000 spectrometer using L_5 (5 cm focal length and diameter). Diaphragms were used throughout the optical path to reduce any stray radiation from the HCL and optical emission from the ICP. The photomultiplier tube (PMT) output from the current-to-voltage amplifier and nanovolt amplifier was acquired by the

lock-in amplifier. The lock-in amplifier was triggered by an external trigger output from the chopper power supply. The optimal slit width (HR1000 monochromator) and PMT high voltage were independently determined for each element studied for an optimal signal-to-noise ratio. Absorption data were collected with a chart recorder.

Sample Preparation. Stock solutions (1000–10000 mg L^{-1} in 2% HNO_3) were obtained from Inorganic Ventures, Inc. (Brock, NJ), for the elements studied. Several synthetic mixtures were made with two to three elements. Working standards were made by serial dilutions of the stock solutions. Distilled, demineralized water (Barnstead Sybron Corp. Boston, MA) was used throughout this work.

Procedure. As discussed previously (*26*), continuum source-ICP-AAS (CS-ICP-AAS) was obtained with the HR1000 set at the fifth order and the predisperser (J-Y H10) set at the first order of the absorption line. Since one complete scan of the photodiode array required 33 ms, 300 data acquisition spectra were averaged for each spectrum for a total acquisition time of 10 s. The transmittance signal of each element was determined as I_a. Although the diaphragms reduced the solid angle of collected ICP emission from the T-shaped bonnet as much as possible from reaching the detector (see Figure 3), any atomic or ionic emission (with the source radiation blocked) that did reach the detector (I_e) was subtracted from I_a. Thus, the transmittance signal for each element was calculated as $I = I_a - I_e$. For each absorption spectrum obtained, a blank spectrum (water aspirated into the ICP) of the incident radiation (I_0) was obtained. The absorption spectrum for each element was determined by $A = \log I_0/I$. All calculations were performed with the supplied OSMA software.

For work involving HCL-ICP-AAS with the T-shaped bonnet, all data were manually manipulated from the chart recorder readings. The light chopper and lock-in amplifier minimized any dc component of emission signals from the ICP. Unlike work with the continuum source, both the J-Y H10 and HR1000 monochromators were operated in first order of the atomic absorption line studied. Blank noise readings were obtained by measuring the peak-to-peak noise on the chart recorder. An instrumental bandwidth of 1 Hz was used. The optimal observation region above the ICP load coil was 27 mm. For both the continuum and line source, the probe beam was directed through the center of the T. This probe beam position seemed the most sensitive for the absorption studies.

Plasma Temperature and Electron Density. Spectroscopic measurements are one of the best means for obtaining spatially and temporally resolved values of temperature and species number densities without perturbing the mechanisms of the plasma or influencing the temperature (*27*, *28*). An accurate knowledge of the plasma temperature can lead to a better understanding of analyte vaporization, dissociation, atomization, and ionization processes (*29*). A spectroscopic emission method was performed where neutral iron was selected as the thermometric species. A factor in the line selection process for iron was based on (i) maximal spread in excitation levels, (ii) freedom from plasma spectral interferences, (iii) availability of accurate transition probabilities, and (iv) wavelength proximity, which eliminates the need for calibrating detector instrumentation response with respect to wavelength (*29*). The wavelengths, excitation energies, statistical weights, and transition probabilities were taken from a reference by Fuhr, Martin, and Wiese (*30*).

Determination of relative electron (number) density was based on the measurement of the Stark broadening of an atomic hydrogen line. The H_β (486.1 nm) line was chosen because it is generally free from plasma spectral interferences, has a sufficient intensity for measurement, and has a small half-width (0.1–0.5 nm) and extensive Stark data are available for this line (*31–33*). Both Doppler broadening and instrumental broadening are usually negligible compared to Stark broadening (*32*). For the results presented in this work, the Doppler half widths were deconvoluted from the total line half widths to obtain the Stark half widths. The Doppler half width had less than a 10% effect on the total line half width.

RESULTS AND DISCUSSION

Absorption Spectra. Unlike conventional line sources, the broad band emission from continuum sources allows one to optically probe both atomic and ionic absorption transitions. The ICP allows efficient atomization and ionization of many elements. The HR1000 high-resolution monochromator was operated in the fifth or fourth order to nearly fully resolve atomic and ionic absorption lines. The use of a photodiode array allowed real time, simultaneous multiwavelength measurements. Figure 5 is an atomic absorption spectrum obtained for 0.5 μg mL^{-1} magnesium. The simultaneous observation of more than one element is shown in Figures 6 and 7. The many absorption lines of nickel in Figure 6 demonstrates the great information gathering power of this technique. In Figures 6 and 7, a spectral window was chosen for the prominent nickel and silver absorption line, respectively. Although cobalt and copper have stronger absorption lines elsewhere, they can still be detected within these chosen spectral windows at the microgram per milliliter level. Figure 8 shows not only a multielement scan for magnesium and manganese but an atomic (Mn) and ionic (Mg) absorption scan as well. The ability to investigate ionic absorption lines of easily ionized elements is an attractive alternative to investigating only atomic absorption lines.

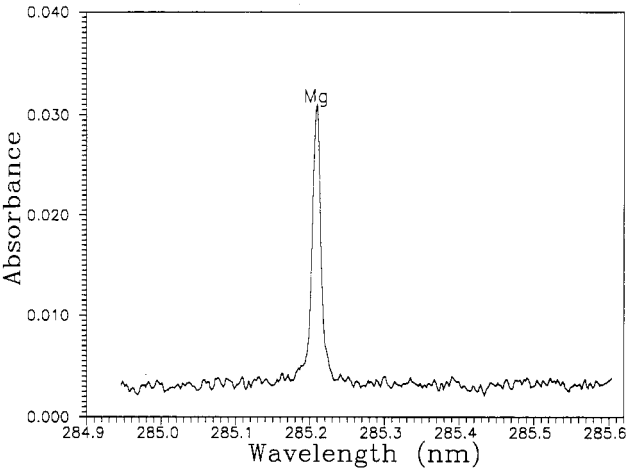

Figure 5. Atomic absorption spectrum of magnesium (0.5 μg mL^{-1}).

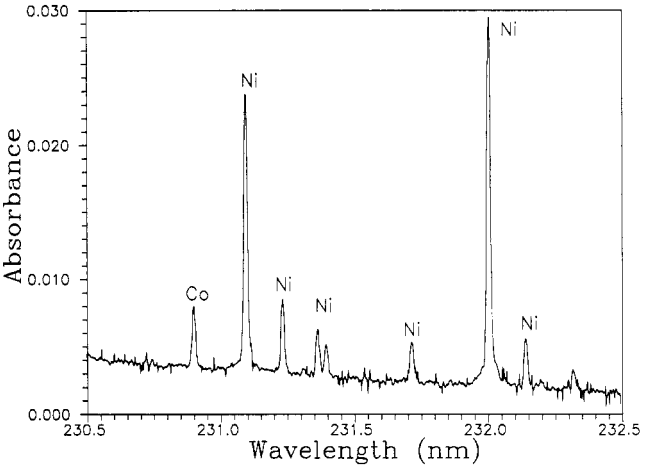

Figure 6. Atomic absorption spectrum of a multielement mixture of nickel and cobalt (100 μg mL^{-1}).

Background Correction and Noise. All spectra shown in Figures 5–8 with the CS-ICP-AAS studies are not background corrected. With the supplied software, the measured absorbance peak height was easily subtracted from a base line that was not positioned at 0.0 absorbance units. For the HCL-ICP-AAS studies, background correction was obtained by subtracting the transmission peak from the blank transmission base-line signal; base-line drift was negligible.

For either study, ICP emission noise was not a significant source of noise. The use of diaphragms significantly mini-

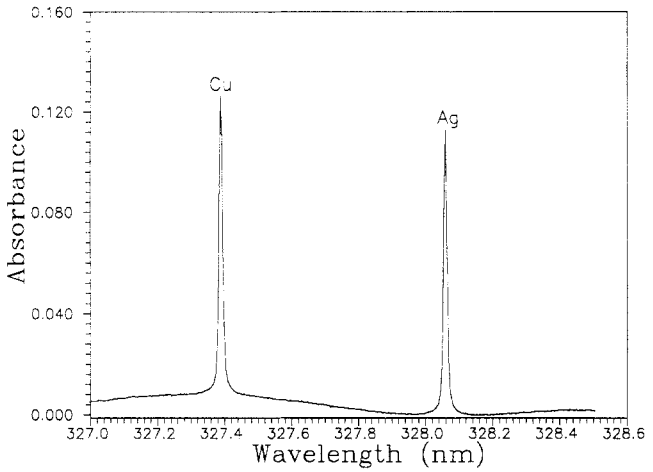

Figure 7. Atomic absorption spectrum of a multielement mixture of copper and silver (100 μg mL^{-1}).

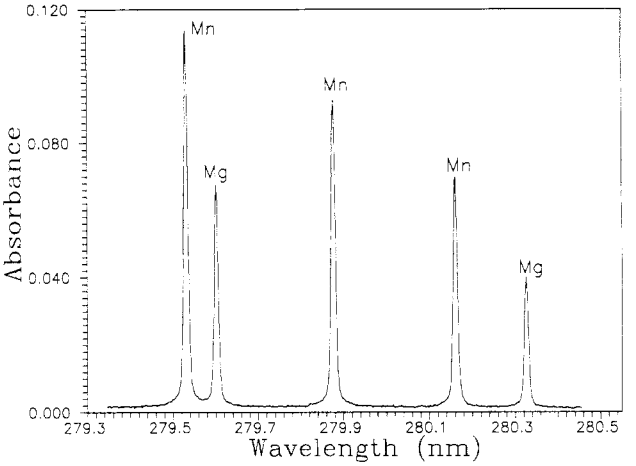

Figure 8. Atomic absorption spectrum showing atomic and ionic absorption of manganese and magnesium (10 μg mL^{-1}), respectively.

Table II. Comparison of Detection Limits for CS-AAS Results

element	λ_{AAS}, nm	sensitivity, μg mL^{-1}	limits of detection, μg mL^{-1}: this work "T-shaped" bonnet	limits of detection, μg mL^{-1}: previous work CS-ICP-AAS[a]	limits of detection, μg mL^{-1}: CS-flame-AAS[b]
Ag(I)	328.1	4	0.2	5	0.007
Ca(I)	422.7	0.2	0.04	3	0.003
Cd(I)	228.8	2	0.5	3	0.03
Co(I)	240.7	2	0.5	10	0.07
Cr(I)	357.9	3	0.6	10	0.02
Cu(I)	324.7	2	0.4	4	0.01
Fe(I)	248.3	2	0.4	8	0.07
Li(I)	670.8	0.07	0.03		0.003
Mg(I)	285.2	0.07	0.01	0.7	0.001
Mn(I)	279.5	0.8	0.2	4	0.01
Na(I)	589.0	0.4	0.06	3	0.003
Ni(I)	232.0	0.3	0.6	10	0.07
Sr(I)	460.7	0.7	0.2	6	0.02
Zn(I)	213.9	10	3	20	0.07
Ba(II)	455.4	10	7	10	*c*
Ca(II)	393.7	20	4	5	*c*
Mg(II)	279.5	0.4	0.07	2	*c*
Mn(II)	257.6	7	4	10	*c*
Sr(II)	407.8	9	5	6	*c*

[a] Taken from ref 26 (a single-pass system). [b] Taken from ref 34 (a single-pass system). [c] Not done.

mized any ICP emission from reaching the detector for the CS-ICP-AAS studies. In general, the probed absorption region within the T-shaped bonnet is a relatively dark region; that is, emission from this region is greatly reduced. Along with the lock-in amplifier, additional rejection of noise was provided by the nanovolt amplifier with its frequency band-pass of 100–300 kHz for the HCL-ICP-AAS studies. Source shot noise from the HCLs was the prominent source of noise. However, with the continuum source, source shot noise was prominent at wavelengths greater than 250 nm, while detector (diode-to-diode) noise became prominent below wavelengths of 250 nm because of the relatively poor emission intensity of the continuum source below 250 nm.

Analytical Figures of Merit. For the CS-ICP-AAS studies, detection limits and sensitivities (the characteristic concentration which would yield a 1% absorption signal) are reported in Table II. As a comparison, detection limits by other work involving single-pass CS-AAS are also given in Table II. The detection limits for this work compared to work performed previously in an ICP (with a conventional torch) (*26*) are at least an order of magnitude better. A likely reason for this improvement involves the increase in absorption path length provided by the T-shaped bonnet. The increase in the atomic absorption signal using the bonnet was almost directly proportional to the increase in absorption path length compared to a conventional torch. Detection limits, however, for the best reported CS-flame-AAS results by O'Haver (*34*), were at least an order of magnitude better than the results obtained in this work with the continuum source. Ionization losses for atomic absorption are more significant in an ICP than in a flame leading to poorer atomic absorption detection limits. Although ionization losses are very significant for atomic absorption using a conventional torch, these losses are not as significant when using the T-shaped bonnet. Obviously, the operation at lower rf powers (compared to a conventional torch) with the bonnet has a direct negative effect on the ionic absorption observed (as seen from the data reported in Table II). The use of O'Haver's modulated continuum source and lock-in detection may improve the sensitivity of this experimental system (*34*).

The detection limits and sensitivities for the HCL-ICP-AAS studies are reported in Table III. The best reported detection limits of line source AAS are also given (*35*). The best absorption signal obtained for the refractory element vanadium

Table III. Operational Parameters and Analytical Figures of Merit

element	λ_{AAS}	HR1000 slits, mm	ICP power, W	HCL-ICP-AAS: sensitivity, μg mL^{-1}	HCL-ICP-AAS: LOD, μg mL^{-1}	HCL-flame-AAS lit. value LOD[a]
Ba(I)	553.5	1.5	400	8	1	0.01
Ca(I)	422.7	1.0	400	0.1	0.03	0.002
Cd(I)	228.8	2.0	400	0.1	0.1	0.001
Mg(I)	285.2	1.0	400	0.05	0.008	0.0003
Mn(I)	279.5	2.0	400	0.7	0.1	0.002
V(I)	318.5	1.5	600	7	4	0.03

[a] Taken from ref 35.

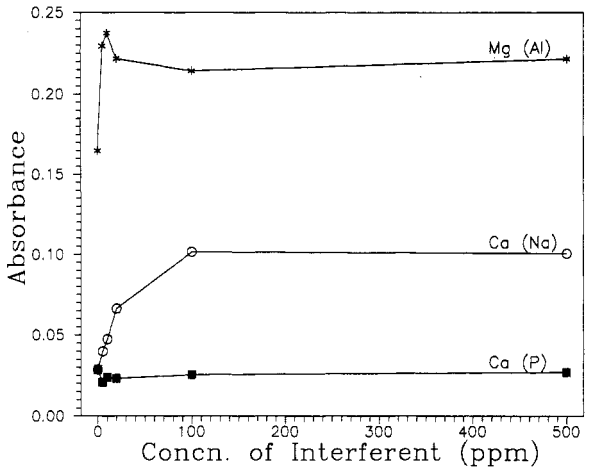

Figure 9. Interferent effects on magnesium and calcium (1 μg mL^{-1}).

was at a higher plasma rf power (i.e., 600 W) compared to the other studied elements. The detection limit obtained for magnesium is competitive compared to commercial AA systems. Overall, detection limits obtained in this work were at least 1 to 2 orders of magnitude poorer than commercial flame-AA values. Again, ionization losses and different limiting noises may explain these differences in detection limits.

Chemical Interferences. We expected that chemical interferences in our plasma system would be markedly reduced compared to flame-AAS. The most serious interferences for magnesium occurs in the presence of other elements that can form stable oxides. Aluminum is known to interfere with magnesium by forming mixed oxides and thus suppressing its absorption signal (*36–38*). Figure 9 shows the effect of adding varying concentrations of aluminum on a 1 μg mL^{-1} solution of magnesium. Instead of a depressed effect, aluminum slightly enhanced the magnesium absorption signal. Further speculation of the enhancement has been deferred until a better understanding of this plasma is made. Figure 9 also shows the effect of interferences on calcium. Calcium in the presence of phosphate produces a stable Ca–P compound removing large numbers of calcium atoms; thus, a severely depressed flame atomic absorption signal results (*39*). With our system, the addition of phosphorus to a 1 μg mL^{-1} solution of calcium had little effect on the absorption signal. Sodium has also been known to be an interferent by enhancing atomic absorption signals due to sodium's ease of ionization and thus shifting the ionization equilibrium in hot flames and ICPs (*40*). A marginal enhancement was observed as sodium slightly enhanced the calcium atomic absorption signal.

Plasma Diagnostics. As described by Kalnicky and Kniseley, the temperature was calculated with the aid of the slope method for several iron (Fe I) emission lines listed by Kalnicky and Fassel (*41*). The temperature determined from this method was 4000 K. The electron density was determined by the calculated half-width of the H_β line as a function of the electron density (*31*). Based on a H_β half-width of 0.07 nm, the electron density corresponds to 2×10^{14} cm^{-3}. The measured electron density has also been used to calculate the electron temperature, $T_{e,LTE}$ (K), assuming local thermodynamic equilibrium. $T_{e,LTE}$ values have been evaluated for the corresponding electron densities by Caughlin and Blades (*42*): The LTE temperature based on the measured electron density corresponds to 6800 K. The difference in this temperature from the emission temperature mentioned above supports nonthermodynamic equilibrium of the plasma.

CONCLUSION

There was very little atomic emission observed within the center of the T of the bonnet. The greatest advantage of this T-shaped bonnet is the ability to optically probe atoms within a fairly dark region. Compared to flames, this is attractive since the background emission is very low. Also compared to flames, chemical interferences were reduced with this plasma setup. LODs for many of the ionic absorption lines (and refractory element atomic absorption lines) would probably improve if the plasma rf power could be increased. However, increasing the rf power currently jeopardizes the structure of our T-shaped bonnet. Low rf operating power allowed prudent operation of the system and prevented the potential of cracking the bonnet.

These preliminary results with the T-shaped bonnet seem promising. The ability to increase the atomic absorption path length and to make use of an excellent atomization cell, such as the ICP for absorption, is very attractive. This increase in absorption path length should increase the atomic/ionic residence times within the path of the optical beam. The bonnet can be used continuously on top of conventional ICP torches making it attractive for commercial use. The ability to probe both atomic and ionic species should improve the multielemental capabilities of this technique. Obviously, a common problem with CS-AAS, is the need for a high-resolution monochromator. An echelle spectrometer with a charge-coupled device would offer good spectral resolution and coverage for multielemental analyses. The use of an ICP with the described T-shaped bonnet in AAS should overcome the "atomizer-related shortcomings" as discussed by Hieftje (*43*). The system described here should provide AAS with a simple to use, easily automated, multielement technique.

Future work will employ the use of an HCL and possibly other line sources as radiation sources with this setup. With the relatively low plasma temperatures determined in this study, the plasma within the middle of the T portion of the bonnet appears to be a very hot inert gas. A smaller inner diameter T-shaped bonnet will be constructed to try and restrict the atoms and ions to a more confined and restricted region: A miniaturized ICP torch may be useful for this application. Mini-ICP torches have been reported to provide the same analytical capabilities and atomization and excitation characteristics as conventional torches, however, at much lower rf powers (*44*, *45*). We may also attempt to simulate the work performed by Fuwa and Vallee but with a conventional ICP torch and its plasma plume directed into one end of a long path absorption tube.

ACKNOWLEDGMENT

Thanks go to Rudi Strohschein and Dick Moshier for their expeditious efforts in constructing several T-shaped bonnets. Support for this work was also funded by a fellowship from British Petroleum of American for M.M. Thanks especially go to Nicolo Omenetto for his stimulating discussions and help concerning the work involved with this system.

LITERATURE CITED

(1) Rubeska, I.; Moldan, B. *Appl. Opt.* **1968**, *7*, 1341.
(2) Fuwa, K.; Vallee, B. L. *Anal. Chem.* **1963**, *35*, 942.
(3) Ando, A.; Fuwa, K.; Vallee, B. L. *Anal. Chem.* **1970**, *42*, 818.
(4) Agazzi, E. J. *Anal. Chem.* **1965**, *37*, 364.
(5) Fassel, V. A. *Science* **1978**, *202*, 183.
(6) Magyar, B.; Aeschbach, F. *Spectrochim. Acta* **1980**, *35B*, 839.
(7) Wendt, R. H.; Fassel, V. A. *Anal. Chem.* **1966**, *38*, 337.
(8) Veillon, C.; Margoshes, M. *Spectrochim. Acta* **1968**, *23B*, 503.
(9) Downey, S. W.; Nogar, N. S. *Appl. Spectrosc.* **1984**, *38*, 876.
(10) Mermet, J. M.; Trassy, C. *Appl. Spectrosc.* **1977**, *31*, 237.
(11) Bordonali, C.; Biancifiori, M. A. *Met. It.* **1967**, *No. 8*, 631.
(12) Biancifiori, M. A.; Bordonali, C. *Com. Naz. Energ. Nucl.* **1967**, *67*, 15.
(13) Greenfield, S.; Smith, P. B.; Breeze, A. E.; Chilton, N. M. D. *Anal. Chim. Acta* **1968**, *41*, 385.
(14) Abdallah, M. H.; Diemiaszonek, R.; Jarosz, J.; Mermet, J. M.; Robin, J.; Trassy, M. *Anal. Chim. Acta* **1976**, *84*, 271.
(15) Umemoto, M.; Kubota, M. *Spectrochim. Acta* **1987**, *42B*, 1053.
(16) Hart, L. P.; Smith, B. W.; Omenetto, N. *Spectrochim. Acta* **1986**, *41B*, 1367.
(17) Uchida, H.; Tanabe, K.; Nojiri, Y.; Haraguchi, H.; Fuwa, K. *Spectrochim. Acta* **1980**, *35B*, 881.
(18) Blades, M. W.; Hieftje, G. M. *Spectrochim. Acta* **1982**, *37B*, 191.

(19) Kornblum, G. R.; De Galan, L. *Spectrochim. Acta* **1977**, *32B*, 71.
(20) Gillson, G.; Horlick, G. *Spectrochim. Acta* **1986**, *41B*, 431.
(21) Uchida, H.; Tanabe, K.; Nojiri, Y.; Haraguchi, H.; Fuwa, K. *Spectrochim. Acta* **1981**, *36B*, 711.
(22) Rybarczyk, J. P.; Jester, C. P.; Yates, D. A.; Koirtyohann, S. R. *Anal. Chem.* **1982**, *54*, 2162.
(23) Nojiri, Y.; Tanabe, K.; Uchida, H.; Haraguchi, H.; Fuwa, K.; Winefordner, J. D. *Spectrochim. Acta* **1983**, *38B*, 61.
(24) Liang, D. C.; Blades, M. W. *Anal. Chem.* **1988**, *60*, 27.
(25) Ng, K. C.; Jensen, R. S.; Brechmann, M. J.; Santos, W. C. *Anal. Chem.* **1988**, *60*, 2818.
(26) Mignardi, M. A.; Jones, B. T.; Smith, B. W.; Winefordner, J. D. *Anal. Chim. Acta*, submitted 1989.
(27) Browner, R. F.; Winefordner, J. D. *Anal. Chem.* **1972**, *44*, 247.
(28) Robinson, D.; Lenn, P. D. *Appl. Opt.* **1967**, *6*, 983.
(29) Kalnicky, D. J.; Kniseley, R. N.; Fassel, V. A. *Spectrochim. Acta* **1975**, *30B*, 511.
(30) Fuhr, J. P.; Martin, G. A.; Wiese, W. L. *J. Phys. Chem. Ref. Data* **1988**, *17*(4).
(31) Wiese, W. L. In *Plasma Diagnostics Techniques*; Huddlestone, R. H., Leonard, S. L., Eds.; Academic Press: New York, 1965; Chapter 6.
(32) Kalnicky, D. J.; Fassel, V. A.; Kniseley, R. N. *Appl. Spectrosc.* **1977**, *31*, 137.
(33) Kirsch, B.; Hanamura, S.; Winefordner, J. D. *Spectrochim. Acta* **1984**, *39B*, 955.
(34) O'Haver, T. C. *Analyst* **1984**, *109*, 211.
(35) Thermo Jarrell Ash Technical Report, 1/88, 5k, Thermo Jarrell Ash: Franklin, MA.
(36) Elwell, W. T.; Gidley, J. A. F. *Atomic Absorption Spectrophotometry*; The Macmillan Company: New York, 1962; Chapter 8.
(37) Menzies, A. C. *Anal. Chem.* **1960**, *32*, 898.
(38) Halls, D. J.; Townshend, A. *Anal. Chim. Acta* **1966**, *36*, 278.
(39) Schrenk, W. G. *Analytical Atomic Spectroscopy*; Plenum Press: New York, 1975; Chapter 2.
(40) Ingle, J. D., Jr.; Crouch, S. P. *Spectrochemical Analysis*; Prentice-Hall: Englewood Cliffs, NJ, 1988; Chapter 7.
(41) Kalnicky, D. J.; Kniseley, R. N. *Spectrochim. Acta* **1975**, *30B*, 511.
(42) Caughlin, B. L.; Blades, M. W. *Spectrochim. Acta* **1984**, *39B*, 1583.
(43) Hieftje, G. M. *J. Anal. Atom. Spectrosc.* **1989**, *4*, 117.
(44) Savage, R. N.; Hieftje, G. M. *Anal. Chem.* **1979**, *51*, 408.
(45) Rezaaiyaan, Y. R.; Hieftje, G. M.; Anderson, H.; Kaiser, H.; Meddings, B. *Appl. Spectrosc.* **1982**, *36*, 627.

RECEIVED for review August 28, 1989. Accepted December 18, 1989. Research supported by NIH-5-R01-GM38434-02.

Mass Spectrometric System for the Measurement of Aroma/Flavor Permeation Rates across Polymer Films

J. C. Tou,* D. C. Rulf, and P. T. DeLassus

The Analytical Sciences Laboratories, The Dow Chemical Company, Midland, Michigan 48667

A mass spectrometric system consisting of a mass spectrometer, a flow-through hollow fiber interface, and a permeation device is developed for the measurement of aroma/flavor permeation rates across polymeric films. The system exhibits parts per billion sensitivity to gaseous organic molecules and, therefore, is capable of determining permeability, diffusivity, and solubility of aroma/flavor constituents in polymeric films with both the feed side and the permeating side at an ambient pressure and the feed concentration down to parts per million level. The response time was found to be less than 1 min when the interface was maintained at 75 °C. The experiments can be performed at a temperature range from subambient to 100 °C. A humidifier system can be connected to the permeation device for an experiment where the humidity effect on the permeation rates is of interest. For films whose diffusivity cannot be determined from the fast rising transient portion of the permeation curve, a desolvation technique is developed from which solubility and therefore diffusivity can be evaluated. Also presented and discussed are the results from two types of the commercial films exhibiting drastically different permeability.

INTRODUCTION

Polymeric materials have become increasingly important in the food packaging industry because of their lighter weight, lower cost, and easier processing than the conventional materials such as glass, steel, and aluminum (*1*). The barrier properties of the polymeric materials against the food aroma/flavor constituents at different conditions are critical to the suitability of such applications. Generally speaking, there are two major channels available for the losses of the aroma/flavor components to the packaging materials. One is the transmission loss due to the permeation of the aroma/flavor molecules across the polymeric films to the environment, and the other is the sorption loss due to the solubility of the aroma/flavor molecules in the polymer. The permeation rate or permeability at normalized conditions depends on both solubility and diffusivity of the molecules in the polymeric films. Both of the losses have an impact on the shelf life of the packaged food. Since useful packaging materials must exhibit very low solubility and diffusivity, the measuring techniques must have high sensitivity. Several techniques have been developed and reported in the literature. Bredeweg and Caldecourt (*2*) reported an electron impact mass spectrometric technique with high sensitivity and specificity for the permeation rate measurements. It requires, however, that the permeating side of a membrane be exposed to high vacuum for mass spectrometric analysis. This requirement may alter the permeation characteristics of a membrane due to possible physical changes resulting from the vacuum seal and support. Zobel (*3*) developed an apparatus based on flame ionization techniques, which is capable of measuring the permeation rates down to about 3×10^{-12} kg·m^{-2}·s^{-1}. Because of the nature of flame ionization, the technique is incapable of measuring the permeation rates of individual components in mixtures. Caldecourt and Tou (*4*) developed two additional techniques based on atmospheric pressure ionization mass spectrometry and photoionization with comparable sensitivity as the flame ionization technique described above. However, the photoionization technique suffers from an additional drawback. The window in the photoionization detector tends to be coated by the photodecomposition products from the permeating molecules resulting in a sensitivity decrease. The atmospheric pressure ionization mass spectrometric technique suffers from its inherently narrow dynamic range and competitive ion–molecular reactions (*5*). Judgement and further validation complicate the operation if the feed is a mixture. Therefore, need still exists for a general and reliable technique for the evaluation of the aroma/flavor permeation across a polymeric

0003-2700/90/0362-0592$02.50/0